ARTICLES

Raman study of phase transition and hydrogen bond symmetrization in solid DCl at high pressure

Eriko Katoh
Core Research for Evolutional Science and Technology, Japan Science and Technology Corporation, Kawaguchi, Saitama 332-0012, Japan

H. Yamawaki, H. Fujihisa, M. Sakashita, and K. Aoki*
National Institute of Materials and Chemical Research, 1-1 Higashi, Tsukuba, Ibaraki 305-8565, Japan and Core Research for Evolutional Science and Technology, Japan Science and Technology Corporation, Kawaguchi, Saitama 332-0012, Japan
(Received 20 May 1999)

Phase transitions in solid DCl have been investigated by Raman spectral measurement up to 70 GPa at 298 K. The I-III phase transition accompanied by orientational ordering of the molecules took place at 19.0 ± 0.5 GPa, exactly the same pressure as observed for solid HCl. A further transition with hydrogen bond symmetrization (III-IV transition) was observed at about 56 ± 2 GPa higher by 5 GPa than the symmetrization pressure of HCl previously determined. The bond symmetrization is realized when the midpoint barrier separating two potential minima along the hydrogen-bonding axis is depressed and smeared out quantum mechanically. The observed isotope effects on the symmetrization pressure are hence interpreted in terms of proton (deuteron) tunneling transfer in the hydrogen bonding potential, which gradually is deformed toward a single minimum shape with increasing pressures.

I. INTRODUCTION

Hydrogen bonding plays a dominant role in molecular arrangement and physical or chemical properties in solids. The bonding nature is characterized by directionality like covalent bonding and proton transfer along the bonds. The former nature is readily recognized in diamondlike structures of ice and the latter in phase transitions such as a ferroelectric-dielectric transition of KDP. The proton, which occupies one minimum of a double-minimum potential under ordinary conditions, can transfer between the two minima separated by a midpoint potential barrier by quantum-mechanical tunneling motion. The frequency of proton transfer depends on the potential shape: the height of midpoint barrier and the distance between two minima. Applying pressure would reduce the barrier height and the minimum-minimum distance and is hence expected to change dramatically the nature of hydrogen bonding. Pressure-induced phase transitions have therefore been investigated for a variety of hydrogen-bonded molecular solids including ice and KDP. In a couple of years, an interest on hydrogen bond symmetrization (proton relocation to the bond midpoint) seems to be growing in experimental[1–4] and theoretical research fields.[5,6]

Hydrogen chloride is a polar diatomic molecule forming hydrogen bonds in solid phases. Three crystalline phases are known to exist at low temperature and ambient pressure.[7–9] The lowest temperature phase (phase III) has an orthorhombic $Cmc2_1$ structure consisting of planar zigzag chains of hydrogen-bonded molecules. Temperature elevation gives rise to transitions from phase III to phase II at 98 K and successively to phase I at 120 K. The phase II has an orthorhombic *Cmca* structure with Cl atoms located essentially in the same positions as those in phase III and H atoms in twofold disordered positions around Cl atoms. In phase I, Cl atoms construct a face-centered-cubic lattice ($Fm\bar{3}m$) with completely disordered protons occupying one of twelve equivalent sites. The sequential transformation from the ordered to disordered structure via the partially disordered one is interpreted as a staged breaking of hydrogen bonds by thermally activated vibrations. The same structural sequence has been observed for HBr at ambient pressure: II-III transition at 90 K and I-II transition at 114 K on heating.

High-pressure phase transitions have been investigated for HCl and HBr experimentally and theoretically. The phase diagram involving I, II, III and plausible I′ phases was determined by Raman and Brillouin scattering measurements in a temperature range of 20–300 K and a pressure range of 0.1 MPa–20 GPa.[10–13] At room temperature, the disordered phase I transformed to the ordered phase III at 19.0 GPa in HCl and at 13.0 GPa in HBr. A further transition into a high pressure phase (phase IV) with symmetrized hydrogen bonds was observed at 51 and 39 GPa for HCl and HBr, respectively, at ambient temperature by Raman measurement up to several 10 GPa.[14,15] The structural stability and vibrational property of solid HBr under pressure were theoretically studied using a first-principle molecular dynamics simulation.[16,17] The calculated results well reproduced the

relative stability between phases I and III and the essential aspects of vibrational states in agreement with the experimental results. Raman and Brillouin measurements revealed that HCl and HBr exhibited a quite similar behavior in phase transition and vibrational property under pressure. One difference found was the stability or instability of symmetric phase. Dissociation reaction from HBr into Br_2 and possibly H_2 was observed immediately after transition to symmetric phase IV in HBr, whereas symmetric phase IV in HCl maintained at least 55 GPa well above the symmetrization pressure of 51 GPa.[14,15]

We have measured Raman spectra of DCl up to 70 GPa at 298 K. The purpose was to investigate the isotope effects on the vibrational states especially associated with the molecular stretching motions along the hydrogen-bonding axis and also on the phase transitions accompanied by molecular reorientation or hydrogen bond symmetrization.

II. EXPERIMENTALS AND RESULTS

Raman spectra of DCl were measured with a piston-cylinder type diamond-anvil cell (DAC). A moving piston and a cylinder body separated in advance for sample loading were cooled in a liquid nitrogen bath below a melting temperature of DCl of 158 K. DCl gas of 99% purity was introduced with a polymer tube to the sample chamber prepared by drilling an about 50 μm hole in a 30 μm thick metal. The gasket material employed was rhenium metal chemically inactive to DCl acid. The separated piston and cylinder were quickly set up and the solidified sample was squeezed in the cooled DAC to several GPa. The DAC was then warmed to room temperature for Raman measurement. The 488-nm line of Ar-gas laser was used for Raman excitation. The scattered lights from the sample were collected in a 180° backscattering configuration and analyzed with a single monochromator. Spectra were recorded with a CCD detector (800×2000 pixels) capable of covering a wave number span of 3000 cm^{-1} with a 2.3 cm^{-1} resolution. Pressure was determined on the basis of the ruby pressure scale proposed for quasihydrostatic condition.[18]

Typical Raman spectra of DCl measured in the pressure range up to 47 GPa are shown in Fig. 1. The second-order Raman peaks of diamond around 2450 cm^{-1} were removed by subtracting a reference diamond spectrum from the raw spectrum. The reference spectrum was taken by moving slightly the laser focusing point from the sample center to a surrounding metal gasket surface. The first-order diamond peak at 1333 cm^{-1} was not satisfactorily removed by the spectrum subtraction. A 1.8-GPa spectrum shows one sharp peak alone at 1986 cm^{-1}, which is attributed to the stretching vibration of DCl molecule. With increase in pressure to about 19 GPa, the stretching peak moves rapidly toward low frequency, becoming a broadened and asymmetric shape. No Raman peak is recognized in the low frequency region down to 200 cm^{-1}, indicating absence of long-range ordering in the molecular arrangement. With the exception of the peak position, the spectral feature is identical to that observed for the low-temperature phase I.[8] The low-pressure phase observed below 19.0 GPa is hence assigned as orientationally disordered phase I with a $Fm\bar{3}m$ cubic structure.

The spectral change associated with I-III phase transition

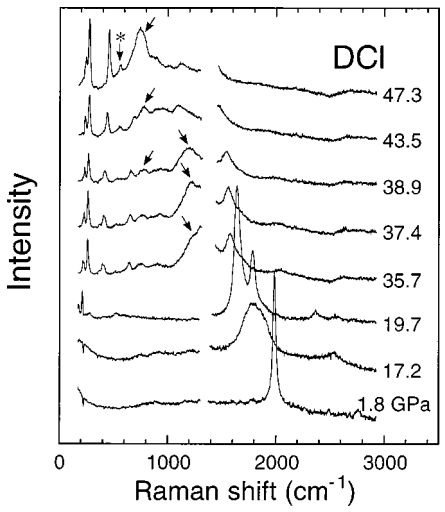

FIG. 1. Raman spectra of DCl measured in the pressure range of 1.8–47.3 GPa. A transition from phase I to III is observed at 19.0 GPa, showing splitting of the stretching peak in the frequency region of 1600–1800 cm^{-1} and appearance of the librational and translational lattice peaks below 1000 cm^{-1}. Dramatic changes in peak intensity due to mixing of vibrational modes are observed in the pressure ranges of 35–39 and 39–47 GPa as marked by arrows. The peaks with asterisks are those from Cl_2 impurity contained in the sample.

is clearly displayed in a spectrum measured at 19.7 GPa. The broadened stretching peak splits into intense, well resolved peaks at 1643 and 1787 cm^{-1}. In addition to the peak splitting, three translational and four librational lattice peaks appear in the frequency regions of 150–400 cm^{-1} and 400–800 cm^{-1}, respectively. These newly appeared lattice peaks tend to move slowly to high frequency with increasing pressure. The spectral changes well correspond to those observed for HCl at the same pressure of 19.0 GPa, being interpreted as a phase transition from cubic $Fm\bar{3}m$ to orthorhombic $Cmc2_1$ structure.[14] The split peaks at 1643 and 1787 cm^{-1} are assigned as an A_1 symmetric and a B_2 antisymmetric stretching mode. The lattice vibrational peaks, which are indistinct in the 19.7-GPa spectrum, become intense and sharp peaks at higher pressures. In a 35.7-GPa spectrum the Raman peaks located at 218, 262, and 403 cm^{-1} may be assigned to A_2, A_1, and B_2 translational modes, and those at 521, 642, 753, and 900 cm^{-1} to A_2, B_1, A_1, and B_2 librational modes, respectively, although there have still been contradictory in peak assignment.[9,17,19,20] The I-III phase transition starting at 18.3 GPa is complete by 19.7 GPa. The transition pressure was determined to be 19.0 GPa by averaging these pressures and found to be in good agreement with the pressure determined from the fluorescence spectrum of an enclosed ruby ball just located by the I-III phase boundary in the sample.

The spectral profile of phase III changes dramatically with increasing pressure, whereby the softening stretching peak invades the librational frequency region below roughly 1200 cm^{-1}. The A_1 stretching peak located at 1643 cm^{-1} just after I-III transition moves to about 1300 cm^{-1} at 35.7 GPa across the diamond peak at 1333 cm^{-1}. A small peak begins to appear at 1226 cm^{-1} in the low frequency side of the stretching peak. This shoulder peak grows rapidly with a slight

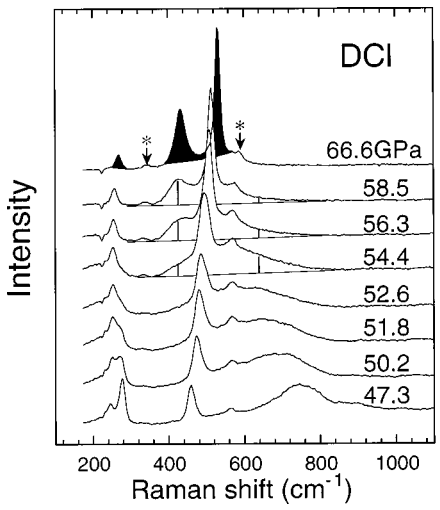

FIG. 2. Raman spectra of DCl measured in the pressure range of 47–67 GPa. Three lattice peaks observed in a 47.3-GPa spectrum are gradually alternated with those of shaded peaks in a 66.6-GPa spectrum. These spectral changes can be interpreted as a phase transition from $Cmc2_1$ to *Cmcm* structure with hydrogen bond symmetrization. The peaks with asterisks are those from Cl_2 impurity contained in the sample.

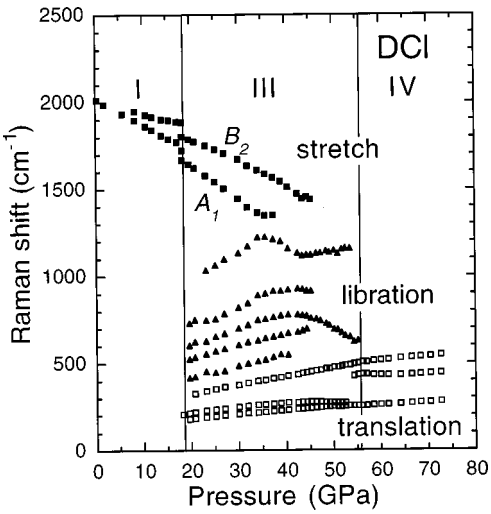

FIG. 3. The variation of Raman frequencies of DCl with pressure. I-III and III-IV phase transitions are readily identified at 19.0 and 56 GPa, respectively. The stretching and librational frequencies are significantly modified owing to mixing of vibrational modes as seen at pressures around 36 and above 43 GPa.

increase in pressure to 38.9 GPa at the expense of the intense stretching peak. Such peak growth is also observed for another librational peak staying steadily at approximately 750 cm^{-1} at pressures between 35 and 50 GPa. This librational peak shows a rapid increase in intensity up to about 50 GPa and a shift toward low frequency down to the translational lattice region above 40 GPa (see also Raman spectra given Fig. 2). These spectral changes are attributed to mixing of the vibrational modes, in the present case, between the softening A_1 stretching and the overtone or fundamental librational modes belonging to the same A_1 symmetry.

Dramatic spectral changes arising from phase transition are observed in the lattice region at pressures of 50–60 GPa (Fig. 2). The A_1 stretching peak located at 657 cm^{-1} at 52.6 GPa gradually disappears during a pressure increase up to 58 GPa, whereas a new peak grows at about 430 cm^{-1}. Changes in the spectral feature are also observed in the region of 200–300 cm^{-1}; the two lattice peaks merge into a single peak at about 58.5 GPa. One peak located around 500 cm^{-1} remains unchanged, showing a continuous shift to high frequency. Eventually, three lattice peaks remain at pressures above 60 GPa and the other peaks originally related to molecular motions such as stretching and rotational vibrations disappear completely. These spectral changes indicate that the phase III transforms to another high-pressure phase (phase IV) likely with a high symmetry structure. The phase transition proceeds sluggishly, starting at 54 GPa and completing at 58 GPa. The transition pressure was hence determined to be 56 ± 2 GPa by taking the midpoint pressure. The spectral feature of phase IV was converted reversibly to those of phase III and phase I with a slight hysteresis in the transition pressures as the pressure was released from 70 GPa, the highest pressure reached, to ambient pressure.

The phase transitions and the vibrational mode mixings are more clearly demonstrated in the frequency vs pressure plots (Fig. 3). Since the stretching peak of disordered phase I was largely asymmetric, it was practically fitted with two peaks to obtain the optimized fitting results. The stretching frequencies of phase I thus obtained show an abrupt drop by roughly 100 cm^{-1} in association with I-III phase transition at 19.0 GPa. The A_1 symmetric and B_2 antisymmetric stretching frequencies continue to decrease, whereas the frequencies of the librational and translational modes are found to increase. It should be noted that a mixing of vibrational modes occurs around 36 GPa, at which the A_1 stretching frequency almost reaches the overtone frequency of libration. The two frequencies, which should have crossed each other around 36 GPa, avoid crossing and separating on further compression. Such unusual behavior arising from vibrational mode mixing is often called as Fermi resonance.[21,22] An anomalous change in frequency is also observed for the fundamental A_1 libration. Its frequency increases monotonically up to 41 GPa and then turns to decrease above it. The III-IV phase transition is clearly identified at 56 GPa. The lattice peaks of phase IV show a slight increase in frequency on further compression to 70 GPa.

The mode mixing results in dramatic changes in peak intensity as well as in vibrational frequency. Integrated peak intensities are plotted as a function of pressure for the A_1 stretching mode and its partners in the mixed states, the overtone and fundamental librational modes, in Fig. 4. The intensity of the stretching peak, which shows pressure-insensitive behavior at low pressures, begins to decrease at about 30 GPa. Synchronously, the intensity of the overtone peak increases by an order of 2 with a further increase in pressure to 37 GPa, reaching a maximum value nearly equal to those of the stretching mode obtained below 30 GPa. The Raman peak with the highest intensity thus seems to be alternated with the overtone peak. The peak intensity of the fundamental libration shows a similar change in intensity, increasing rapidly in the pressure region of 40–47 GPa at the expense of the peak intensity of the overtone libration. The highest

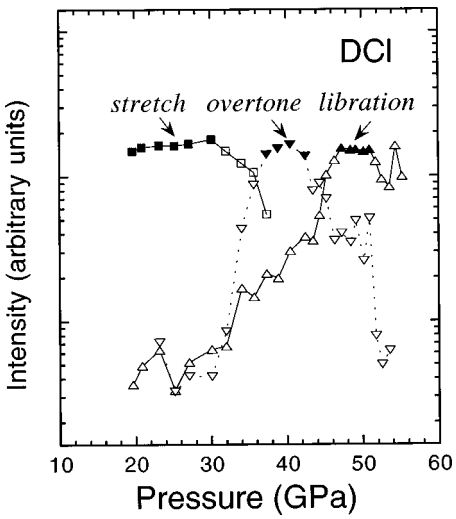

FIG. 4. The variation of the peak intensities of stretching and librational modes with pressure. The overtone and fundamental A_1 librational modes are mixed with and converted into the A_1 stretching mode at pressures where the peak intensities become equal to those of the unmixed A_1 stretching peak below 30 GPa.

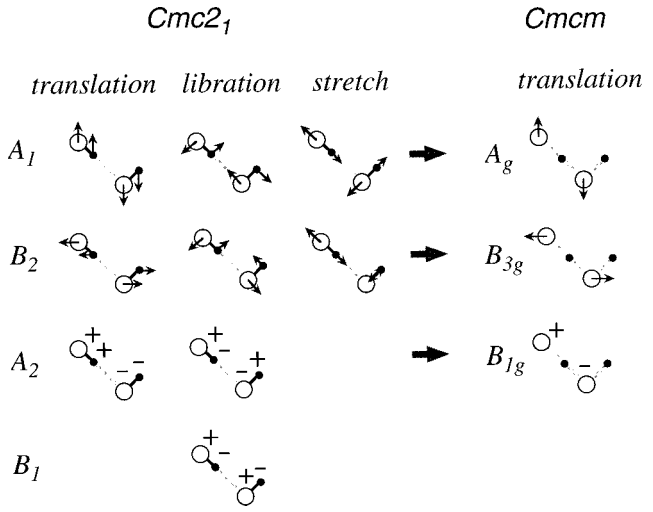

FIG. 5. Raman active vibrational modes for the $Cmc2_1$ (phase III) and *Cmcm* (phase IV) structures of H(D)Cl. Both the structures contain two molecules in the primitive lattices.

intensity peak seems again to be alternated with the A_1 librational peak in the pressure range of 47–51 GPa. The intensity change was shown to be explained in terms of the mixing ratio of coupled vibrational modes.[21]

III. DISCUSSION

The III-IV transition observed at 56 GPa is interpreted in terms of hydrogen bond symmetrization. In the symmetrized phase, the D atoms should occupy the midpoints between the neighboring Cl atoms in the zigzag chains. The centering of the D atoms changes the space group of crystal structure from $Cmc2_1$ to *Cmcm* and consequently the vibrational states. A factor group analysis predicts three translational lattice modes with Raman activity for both $Cmc2_1$ and *Cmcm* structures and additional four librational and two stretching modes for the $Cmc2_1$ structure. Approximate vibrational motions are drawn for the fundamental vibrational modes in Fig. 5. The spectral changes associated with III-IV transition are definitely in agreement with those predicted from the factor group analysis; the Raman peaks related to the rotational and stretching motions of DCl molecule disappear and the translational lattice peaks remain as already shown in Figs. 2 and 3. The remaining three lattice peaks, which are presented by dark shaded peaks in a 66.6-GPa spectrum, provide an evidence of formation of the symmetrized hydrogen bonds in phase IV. A phase transition with hydrogen bond symmetrization has also been observed for solid HCl by Raman measurement.[14] The transition pressure determined from the spectral change was 51 GPa slightly lower than that determined for DCl in the present measurement.

The pressure variation of the stretching frequency provides more detailed insight into the symmetrization process. The stretching modes show clearly a softening behavior in phase I and III (Fig. 3). Above 40 GPa, the frequencies are modified significantly owing to the vibrational mode mixing. The unperturbed or bare frequencies would be derived from the observed mixed-state frequencies by analyzing them using a simple resonance model[21] or a mode coupling model.[22] We can, however, distinguish readily the unmixed or ''purely'' stretching states from the mixed states with the aid of the measured Raman intensity.[15] As shown in Fig. 4, the overtone and fundamental librational modes are converted into the A_1 stretching mode in the pressure regions of 37–43 GPa and 47–51 GPa, respectively. The integrated intensities of the Raman peaks originally assigned as the overtone and fundamental librational modes become nearly equal to those of the stretching mode measured at low pressures below 30 GPa. This consideration allows us to select the purely stretching vibrations as represented with solid symbols in Fig. 4. The stretching frequencies thus selected are plotted as a function of pressure in Fig. 6 along with those of HCl (Ref. 14) by following the same procedure. It is noted here that the DCl stretching frequencies are corrected for mass difference using the relation, $\nu_{\mathrm{HCl}}/\nu_{\mathrm{DCl}}=(m_{\mathrm{D}}/m_{\mathrm{H}})^{1/2}[(m_{\mathrm{H}}+m_{\mathrm{Cl}})/(m_{\mathrm{D}}+m_{\mathrm{Cl}})]^{1/2}$ nearly equal to $\sqrt{2}$. Their uncorrected frequencies can be read from the axis of ordinates on the right. The pressure behavior of the stretching frequency is found to be quite similar between HCl and DCl, showing a rapid decrease in frequency up to about 50 GPa and deceleration above it.

The softening behavior of the stretching vibration is interpreted as arising from shape changes in the hydrogen bonding potential with pressure. The vibrational state of proton in one-dimensional potential deforming from a double to a single minimum shape has numerically been calculated using a generalized double Morse potential.[23] The essential features of the calculated results are illustrated in Fig. 7. The potential minima are well separated from each other by a midpoint barrier and the vibrational states localized at one minimum are approximately described by the harmonic oscillation model [Fig. 7(a)]. The stretching peak frequencies measured by Raman scattering correspond to an excitation from the ground to first excitation level. Depression of the midpoint barrier by applying pressure causes energy-level

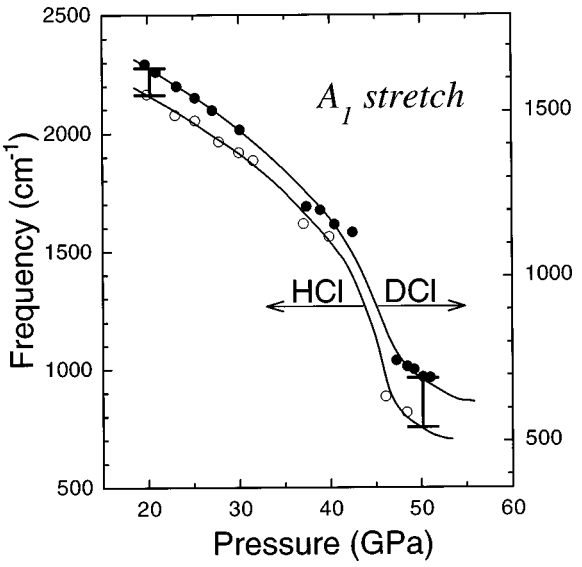

FIG. 6. The variation of purely stretching frequency with pressure. Open and solid circles represent the frequencies of HCl and DCl, respectively. Those of DCl were corrected for atomic mass difference (see text). The axis of ordinates on the right gives their uncorrected frequencies. The solid lines are drawn for the guides to eyes.

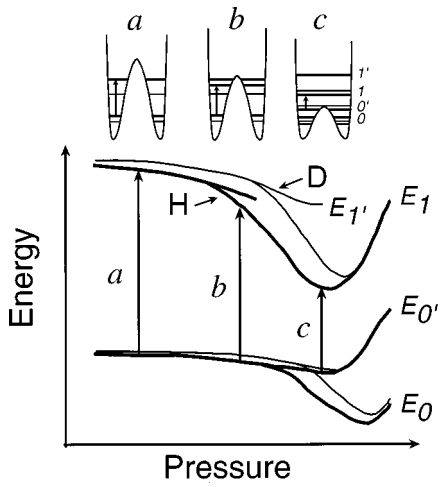

FIG. 7. The pressure variation of hydrogen bonding potential and proton (deuteron) vibrational states are schematically drawn on the basis of the calculated results (Ref. 23). The thick and thin curves represent the energy levels of proton and deuteron vibrations, respectively. In the energy vs pressure curves, the deuteron vibrational energies are supposed to be corrected for mass difference by a factor of about $\sqrt{2}$ to allow immediate comparison with those of proton vibration.

splitting in the first excitation state [Fig. 7(b)]; the excited vibrational state with an energy even below the barrier top can split into 1 and $1'$ levels owing to proton tunneling. Energy level splitting occurs successively in the ground state when the barrier top is further depressed to its energy level, which splits into 0 and $0'$ levels again owing to proton tunneling [Fig. 7(c)]. The observed Raman frequencies correspond here to the $0'-1$ excitation energy. The vibrational energy levels thus changed are schematically drawn for proton vibration (thick line) and for deuteron vibration (thin line) in the bottom of Fig. 7. It should be noted that the vibrational energies of deuteron are corrected again here for mass difference to allow immediate comparison with those of proton.

The isotope effects on the stretching vibration are clearly seen in Fig. 6. The frequencies of proton vibration are located below those of deuteron vibration over the whole pressure range measured. Careful investigation reveals that frequency difference becomes large as the pressure increase: about 126 cm^{-1} in frequency at 20 GPa and about 230 cm^{-1} at 50 GPa. The isotope substitution may influence the stretching vibration through both anharmonicity and tunneling; the former would be dominant at low pressures and the latter at high pressures. At low pressures roughly below 40 GPa, proton (deuteron) oscillates at the bottom of one minimum well approximated with a quadratic form [see Fig. 7(a)]. However, the actual potential curve would deviate downward from the ideal quadratic or harmonic curve as the energy rises apart from the bottom toward the barrier top. This anharmonicity leads to lowering of the first excitation level of proton vibration largely compared to that of deuteron vibration, since the former has an energy level about $\sqrt{2}$ times as high as the latter. The anharmonicity in the potential thus explains the frequency difference between HCl and DCl in the rather low-pressure region.

The increased difference in the stretching frequency at higher pressure can be explained in terms of tunneling effects. As displayed in Fig. 7, the first excitation and ground states show successively energy splitting owing to tunneling transfer of proton (deuteron). The *S*-shape variation of the frequency with pressure (see again the solid curves in Fig. 6) can qualitatively be explained in terms of tunneling effects. The tunneling splitting will take place earlier in proton vibration than in deuteron vibration as shown for the first excitation state [Fig. 7(b)] and the ground state [Fig. 7(c)]. The earlier $0-0'$ splitting in proton vibration, for example, results in a faster decrease in the $0'-1$ excitation energy and hence in the Raman stretching frequency. This is exactly what we have found in the frequency-pressure relations at pressures around 45 GPa (Fig. 6); the stretching frequency of HCl falls slightly earlier than that of DCl to produce a large frequency difference of about 230 cm^{-1} at 50 GPa. The energy diagram in Fig. 7 also gives an explanation to a gradual decrease in Raman intensity observed for the stretching peak in association with III-IV phase transition. For the $0'-1$ Raman excitation, the peak intensity is related to the population of the initial state of $0'$ level, $[\exp(E_{0'}/kT)-1]^{-1}$. The increase in the $0-0'$ splitting reduces the population of $0'$ level and consequently the Raman intensity associated with the $0'-1$ excitation. The Raman peak originating from the stretching vibration exhibits a rapid decrease in intensity near the symmetrization pressure in HCl compared with DCl. This can be attributed to the large tunnel splitting produced in proton vibration.

IV. SUMMARY

The phase transitions in DCl were investigated by Raman measurement up to 70 GPa and at 298 K. The I-III transition accompanied by ordering in molecular orientation took place

at 19.0 ± 0.5 GPa in agreement with that previously observed for HCl. The III-IV transition characterized by symmetrization of the hydrogen bonds was observed at 56 ± 2 GPa higher by 5 GPa than that of HCl. The difference in symmetrization pressure was qualitatively explained in terms of tunneling transfer in the hydrogen bonding potential, which gradually changes from a double to a single minimum shape with increasing pressure.

ACKNOWLEDGMENTS

We gratefully acknowledge Drs. K. Terakura, T. Ikeda, and M. Sprik for helpful discussion on the transition mechanism in hydrogen halides. This work has been supported by Core Research for Evolutional Science and Technology (CREST) Program conducted by Japan Science and Technology Corporation (JST).

*Author to whom the correspondence should be addressed. Electronic address: aoki@home.nimc.go.jp

[1] K. Aoki, H. Yamawaki, M. Sakashita, and H. Fujihisa, Phys. Rev. B **54**, 15 673 (1996).
[2] A. F. Goncharov, V. V. Struzhkin, M. S. Somayazulu, R. J. Hemley, and H. K. Mao, Science **273**, 218 (1996).
[3] E. Wolanin, Ph. Pruzan, J. C. Chervin, B. Canny, M. Gauthier, D. Häusermann, and M. Hanfland, Phys. Rev. B **56**, 5781 (1997).
[4] P. Loubeyre, R. LeToullec, E. Wolanin, M. Hanfland, and D. Hausermann, Nature (London) **397**, 503 (1999).
[5] M. Benoit, D. Marx, and M. Parrinello, Nature (London) **392**, 258 (1998).
[6] M. Bernasconi, P. L. Silvestrelli, and M. Parrinello, Phys. Rev. Lett. **81**, 1235 (1998).
[7] E. Sándor and R. F. C. Farrow, Nature (London) **14**, 171 (1967).
[8] J. E. Vesel and B. H. Torrie, Can. J. Phys. **55**, 592 (1977).
[9] A. Anderson, B. H. Torrie, and W. S. Tse, J. Raman Spectrosc. **10**, 148 (1981).
[10] R. C. Hanson and A. Katz, *High Pressure Science and Technology: Proceedings of the 9th AIRAPT Conference, 99* (North Holland, New York, 1984).
[11] P. G. Johannsen, W. Helle, and W. B. Holzapfel, J. Phys. C **8**, 199 (1984).
[12] T. Kume, T. Tsuji, S. Sasaki, and H. Shimizu, Phys. Rev. B **58**, 8149 (1998).
[13] H. Shimizu, K. Kamabuchi, T. Kume, and S. Sasaki, Phys. Rev. B **59**, 11 727 (1999).
[14] K. Aoki, E. Katoh, H. Yamawaki, M. Sakashita, and H. Fujihisa, Physica B **265**, 83 (1999).
[15] E. Katoh, H. Yamawaki, H. Fujihisa, M. Sakashita, and K. Aoki, Phys. Rev. B **59**, 11 244 (1999).
[16] T. Ikeda, M. Sprik, K. Terakura, and M. Parrinello, Phys. Rev. Lett. **81**, 4416 (1998).
[17] T. Ikeda, M. Sprik, K. Terakura, and M. Parrinello, J. Chem. Phys. **111**, 1595 (1999).
[18] H. K. Mao, J. Xu, and P. W. Bell, J. Geophys. Res. **91**, 4673 (1986).
[19] M. Ito, M. Suzuki, and T. Yokoyama, J. Chem. Phys. **50**, 2949 (1969). They adopted $Bb2_1m$ space group in the vibrational mode analysis of phase III instead of $Cmc2_1$ space group adopted in the present work. The choice of $Bb2_1m$ space group alternates the B_1 and B_2 modes of $Cmc2_1$ structure with the B_2 and B_1 modes, respectively.
[20] J. Obriot, F. Fondére, and Ph. Marteau, J. Chem. Phys. **79**, 33 (1983).
[21] K. Aoki, H. Yamawaki, and M. Sakashita, Science **268**, 1322 (1995).
[22] V. V. Struzhkin, A. F. Goncharov, R. J. Hemley, and H. K. Mao, Phys. Rev. Lett. **78**, 4446 (1997).
[23] P. G. Johannsen, J. Phys.: Condens. Matter **10**, 2241 (1998).